Environ Ecol Stat (2008) 15:265–277
DOI 10.1007/s10651-007-0059-3

Hazards, spatial transmission and timing of outbreaks in epidemic metapopulations

Ottar N. Bjørnstad · Bryan T. Grenfell

Received: 1 May 2005 / Revised: 1 October 2005 / Published online: 6 December 2007

Abstract Highly infectious, immunizing pathogens can cause violent local outbreaks that are followed by the agent's extinction as it runs out of susceptible hosts. For these pathogens, regional persistence can only be secured through spatial transmission and geographically asynchronous epidemics. In this paper we develop a hazard model for the waiting time between epidemics. We use the model, first, to discuss the predictability in timing of epidemics, and, second, to estimate the strength of spatial transmission. Based on the hazard model, we conclude that highly epidemic pathogens can at times be predictable in the sense that the waiting-time distribution between outbreaks is probabilistically bounded; The greater the spatial transmission the more periodic the outbreak dynamics. When we analyze the historical records of measles outbreaks in England and Wales between 1944 and 1965, we find the waiting-time between epidemics to depend inversely on community size. This is because large communities are much more tightly coupled to the regional metapopulation. The model further help identify the most important areas for spatial transmission. We conclude that the data on *absence* of these pathogens is the key to understanding spatial spread.

Keywords Measles · Inter-epidemic periods · TSIR model · Disease ecology · Population dynamics

O. N. Bjørnstad (✉)
Department of Entomology, Pennsylvania State University, University Park, PA 16802, USA
e-mail: onb1@psu.edu

O. N. Bjørnstad · B. T. Grenfell
Center for Infectious Disease Dynamics, Department of Biology, Pennsylvania State University, University Park, PA 16802, USA

O. N. Bjørnstad · B. T. Grenfell
Fogarty International Center, National Institutes of Health, Bethesda, MD 20892, USA

1 Introduction

Acute, immunizing pathogens result in death or recovery of the host and immune-mediated resistance to future reinfection. When these disease agents enter a local community they spark epidemics that deplete the pool of susceptibles until the chain of transmission is broken and the pathogen goes locally extinct. *Ultimately, such* pathogens can only persist within the *metapopulation* setting. [The notion of a metapopulation, here, is taken from theoretical ecology: a collection of largely independent populations (and, in our context, host communities) linked by relatively infrequent inter-migration (with respect to the organism in focus; here the pathogen).] Following local extinction, the susceptible population will build up—from births and, possibly, loss of immunity in previously immunized hosts—until (a) the pathogen is reintroduced through spatial transmission from some other community *and* (b) the local susceptibles have grown numerous enough for any index case to spark off a new chain of transmission. Regional ('metapopulation') persistence requires the rate of replenishment of susceptibles to be adequate *and* the rate of spatial transmission, through the movement of susceptible and infected hosts, to be adequate. Quantifying the rates of spatial transmission ('spatial coupling'), therefore, is a critical challenge in epidemiology because both spread and persistence depends on the coupling of local populations (Keeling et al. 2004). This, incidentally, echoes a contemporary theme in population ecology (Hanski and Gaggiotti 2004).

Among the most infectious of human pathogens are many of the so-called *childhood diseases*, of which measles is an example (Fine and Clarkson 1982; Anderson and May 1991). Innately, children are not necessarily much more susceptible than adults, but the high contagiousness and strong immune-stimulation of these agents result in a low age of infection. As a consequence, transmission in the pre-vaccination era was largely amongst children. The local epidemic dynamics of this class of pathogen have received much attention, and several studies have revealed a close match between theoretical predictions and epidemiological surveillance data, notably for measles and whooping cough. Moreover, the study of their spatial spread comprise an extensive literature in epidemiology, ecology, geography, and statistics (Bartlett 1956, 1957, 1960; Murray and Cliff 1975; Cliff et al. 1993; Xia et al. 2004). Still, much remains to be discovered, both about the patterns and determinants of spatial transmission, and—as is the focus of this paper—the statistical methods that may be used to explore them. In this study we use a stochastic SIR (susceptible-infected-recovered) model (Bjørnstad et al. 2002) to develop an estimator for spatial transmission of measles among populations in the United Kingdom.

Spatial coupling is fundamental to the dynamics and management of several acute animal and human pathogens (Keeling and Rohani 2002; Smith et al. 2002; Keeling et al. 2004). Yet, during the course of outbreaks in well-mixed local populations, the epidemic trajectory of measles will be virtually unaffected by immigrant infection; Indeed, Bjørnstad et al. (2002) calculated that measles epidemics run according to their deterministic course, as soon as there is a handful of local infectious individuals. [We note that this is a nontrivial 'emergent' property of measles' dynamical clockwork; immigration, perturbations and stochasticity have been shown to have significant effects in other childhood infections (Rand and Wilson 1991; Rohani

et al. 2002)]. Hence, data richness—in the sense of numerous mortality and morbidity reports—certainly holds the key to estimation of *local* transmission dynamics (Finkenstadt and Grenfell 2000; Bjørnstad et al. 2002; Finkenstädt et al. 2002). However, such reports do not tell us much with respect to *spatial transmission*; for this, the binary measure of pathogen absence and presence holds crucial information.

Bartlett (1956) discussed how the interepidemic period—the so-called *fade-out length*—in small communities depends critically on the spatial transmission rate. In the following, we first quantify how the interepidemic period is determined by two waiting-time processes: (i) the build-up of local susceptibles and (ii) spatial transmission. We validate the resultant predictions of how the probability of initiating a new epidemic depends on both local susceptible numbers and regional infectives (i.e. the size of the pathogen donor community) using nonparametric regression. Finally, we show that the associated probability of sparking new epidemics, can be used for maximum likelihood estimation. Because we focus on measles, we open with a preamble summarizing the current understanding of measles dynamics.

2 Preamble

Within the field of population dynamics and quantitative epidemiology, measles has become a prototype. There are at least two reasons for this: (1) the simple dynamical clockwork of measles and (2) the excellence of data-recording. The first relates to how measles has no alternative host and no functional strain structure (there are many different viral variants, but cross-immunity appears to be perfect). The second, results partly from how measles is easily diagnosed, and partly from measles historically being a dangerous and highly contagious infection that was subjected to mandatory notification. In England and Wales detailed surveillance protocols were put in place around 1940. In what follows we will focus our analysis on the data collected between 1944 and the onset of mass-vaccination in 1967 in the urban centers (954 cities and towns) of England and Wales. These records are particularly complete as incidence was recorded for each week and each community separately. During this period there is a well-characterized under-reporting bias of about 40–55% (Fine and Clarkson 1982; Bjørnstad et al. 2002; Finkenstädt et al. 2002). The unreported cases are due to the rare miss-diagnosis and the more common failure to seek medical attention. From a strictly statistical perspective, these reports are unlikely to be missing 'completely at random', yet the observational process appears to approximate a simple binomial filter (Clark and Bjørnstad 2004), so any biases are likely to be relatively weak. Barring the under-reporting, however, the records are complete, and testify to spectacular outbreaks of infection. Except for less than a handful of cities (>300 thousand inhabitants) among the almost thousand locations, historical measles incidence exhibited periods of intermittent extinction. Regional persistence, therefore, hinged on episodic reintroduction and spatial transmission.

In light of this, we have previously developed a discrete-time stochastic model—the so-called TSIR model—for the local dynamics of measles (Finkenstadt and Grenfell 2000; Bjørnstad et al. 2002; Grenfell et al. 2002). In any given location, j, we denoted number of infected individuals at time t by $I_{t,j}$, the number of susceptible individuals

by $S_{t,j}$, and the transmission rate by $\beta_{u,j}$. The subscript u signifies that transmission may depend on seasonal variation in aggregation of susceptible and infected children (Fine and Clarkson 1982), so that the force of infection experienced by each local susceptible individual due to local transmission is $\phi_{t,j} = \beta_{u,j} I_{t,j}^{\alpha}$. The exponent α allows for nonlinearities in contact rates that may arise because of nonhomogenous mixing (Liu et al. 1986), as well as the discrete-generation approximation of a more continuous infection model (Glass et al. 2003). The expected number of infected individuals, $\lambda_{t,j}$ arising from local transmission in pathogen generation $t+1$ is then $\lambda_{t,j} = \beta_{u,j} I_{t,j}^{\alpha} S_{t,j}$. The time step is the *epidemic generation length* (= latent + infectious period ≈2 weeks for measles).

Our previous analysis of local dynamics indicates that transmission rates scale in a so-called *frequency-dependent* manner between populations of different size (Bjørnstad et al. 2002). That is, seasonally averaged transmission rate $\overline{\beta_j}$ are inversely proportional to population size according to (see Bjørnstad et al. 2002: Fig .7a): $\log(\overline{\beta}) = 3.64 - 1.02 * \log(N_j)$ ($R^2 = 0.95$). In terms of local transmission, it is therefore sometimes useful to consider the dynamics in terms of the proportions of the local population that are susceptible, $x_{t,j} = S_{t,j}/N_j$, and infected, $y_{t,j} = I_{t,j}/N_j$.

In an epidemic metapopulation, there will—in addition to the strictly local production—be some infections that arise from the contact between local susceptibles and infectious individuals elsewhere. With this in mind, it is natural to modify the equation for the expected incidence as (Bjørnstad et al. 2002; Xia et al. 2004):

$$\lambda_{t,j} = \beta_{u,j} (I_{t,j} + \iota_{t,j})^{\alpha} S_{t,j}, \tag{1}$$

where ι represents infection that arose from spatial contagion.

The growth of an epidemic will be stochastic according to some generalized birth-and-death processes (Bartlett 1956). Approximating the trajectory of measles as a piecewise constant (at the one-generation scale) birth-and-death process, the expectation, λ, will be realized according to (Kendall 1949; Bjørnstad et al. 2002):

$$I_{t+1,j} \sim \text{NegBin}(\lambda_{t,j}, I_{t,j} + \iota_{t,j}), \tag{2}$$

where NegBin(a, b) signifies a Negative Binomial process, with expectation a and clumping parameter b. This follows from assuming a birth-and-death process with a *per capita* growth rate, which in our case is $\lambda/(I + \iota)$. Then starting with *one* infected individual, the number of individuals one-generation later will be distributed according to a geometric distribution with expectation $\lambda/(I + \iota)$. From $I + \iota$ individuals we get a sum of $I + \iota$ geometrics, from which Eq. 2 follows.

The associated balance equation for the susceptibles is:

$$S_{t+1,j} = S_{t,j} + BN_{t,j} - I_{t+1,j}, \tag{3}$$

where B is the *per capita* birth rate. Note that these equations ignore mortality because both case fatality from measles and child/adolescent mortality rates have been very low in developed nations during recent times.

The number of susceptibles, $S_{t,j}$—and thereby the proportion of susceptible, $x_{t,j}$—is not directly observed. However, we can reconstruct these variables by rewriting the recursive equation (3) according to Finkenstadt and Grenfell (2000):

$$S_{t,j} = \overline{S}_j + D_{0,j} + \sum_{k=0}^{t} BN_{k,j} - \sum_{k=0}^{t} I_{k,j}/\rho, \tag{4}$$

where $\overline{S}_j$ is the mean number of susceptibles of community j, $D_{0,j}$ is the unknown deviations around the mean at time 0, and ρ is the reporting rate. This rate was around 50% in England and Wales during the prevaccination era ($\overline{\rho} = 0.52$, SE $= 0.01$) (Bjørnstad et al. 2002). We can reconstruct the time series $D_{t,j}$ of how the local susceptible numbers deviate from the local mean value, $D_{t,j} = S_{t,j} - \overline{S}_j$, by rewriting (4) as,

$$\sum_{k=0}^{t} BN_{k,j} = D_{0,j} + 1/\rho \sum_{k=0}^{t} I_{k,j} + D_{t,j}, \tag{5}$$

from which it is clear that $D_{t,j}$ is the residual from the regression of cumulative number of births on the cumulative number of cases. Note, that this reconstruction still works when $D_{0,j}$ and the reporting rate ρ is unknown because these are accommodated by the intercept and slope of the cumulative-cumulative regression. The method does not allow the independent estimation of the mean number (or mean proportion) of susceptibles. However, previous analyses estimated the mean proportion of susceptibles to be around 4% (although it may be as large as 5–8%) (Bjørnstad et al. 2002).

In our previous study (Bjørnstad et al. 2002; Grenfell et al. 2002), we found that the full stochastic model (1–3) applied to the endemic portions of the time series (i.e. $I_{t,j} > 0$) gave narrow parameter estimates and encouraging long-term prediction of the epidemic trajectories.

Except for around ten cities that were above the 'critical community size' (ca. 250,000–300,000), the local dynamics of measles is critically dependent on reintroductions following local extinctions (as the infectious agent burns through and uses up the susceptible population) (Bartlett 1960; Grenfell and Harwood 1997). Given the limitation of endemic dynamics for quantifying spatial coupling (Finkenstädt et al. 2002; Bjørnstad et al. 2002), it is natural to focus on the extinction-recolonization process. Thus while previous time series modelling provided insight into measles cycles and epidemics, it left the central questions of spatial coupling open. In this study, we explore the relationship between local fade-outs and spatial transmission.

3 Theoretical hazards and waiting times

Following extinction, the local dynamics are converted into waiting time processes, for which the probability that the fade-out will end (the hazard) is governed by (a) the probability of contact between local susceptibles and regional infectives, and (b) the probability that a local epidemic will result from such an event (Bartlett 1956). During this period, the number of local susceptibles is building up due to births:

$$S_{t+1,j} = S_{t,j} + BN_j. \tag{6}$$

Spatial contact, therefore, depends on the probability that an individual from location j is susceptible (given by the proportion of susceptiblity, $x_{t,j}$), the probability that a non-local individual is infectious, $\overline{y}_t = \sum_{k\neq j} I_{t,k} / \sum_{k\neq j} N_j$, and the spatial isolation, $1/c_j$, where c_j is a measure of spatial coupling of community j to all other communities. Obviously, the probability that no spatial contacts will occur in a given time step will be $\exp(-c_j x_{t,j} \overline{y}_t)$. For relatively weak coupling, we may assume $\iota \sim \text{Bin}(1, 1 - \exp(-c_j x_{t,j} \overline{y}_t))$, though other formulations are possible (Xia et al. 2004).

Given a spatial contact, there will be a probability $1/(1+\beta_{u,j} S_{t,j})$ that *no* epidemic will result: the null probability of Eq. 2 when $I_{t,j} = 0$ and $\iota_{t,j} = 1$. A new epidemic will be sparked by the complementary probability, so that the discrete-time hazard $\hbar$ is the probability of the joint occurrence of this event and the occurrence of a spatial contact:

$$\hbar(t, j) = \frac{\beta_{u,j} S_{t,j} (1 - \exp(-c_j x_{t,j} \overline{y}_t))}{1 + \beta_{u,j} S_{t,j}}, \tag{7}$$

which is an increasing function in the number of local susceptible, S_j, and the proportion of non-local individuals that are infectious, $\overline{y}$. It may further depend on population size, if isolation is size dependent. Notice further that because the local susceptible population builds up through time, the hazard asymptotes to the spatial contact probability.

We previously carried out a detailed analysis of the seasonal transmission rate $\beta_{u,j}$ in 60 communities that span three orders of magnitude in population size (Bjørnstad et al. 2002). The transmission rate was found to vary widely through the season (see Bjørnstad et al. 2002: Fig. 7b) reflecting the well-known dependence of transmission on school contact rates (Fine and Clarkson 1982). The transmission rate varied by a factor of 3.0 (median = 2.7, se = 0.22) through the season. At the same time, the variation in proportion of infected varied by a factor of around a hundred through the epidemic cycle (mean = 111.7, median = 71.7, se = 17.3).

The theoretical waiting time distribution between outbreaks—which also represents the probability density function for a fade-out of length T—is given by the *hazard waiting time*, W:

$$W(T, j) = \hbar(T, j) \prod_{t=1}^{T-1} 1 - \hbar(t, j), \tag{8}$$

where $\hbar(t, j)$ is as given in Eq. 7. [Readers familiar with survival analysis will recognize (8) as $\hbar(T, j)(1 - H(T - 1, j))$, where H is the integrated hazard.] This distribution depends critically on how strongly each local community is coupled to the regional population (Fig. 1a). With strong spatial coupling, the mode of the waiting-time distribution can be close to zero. Weakly coupled communities, in contrast, may wait as much as a year (or more) between outbreaks; the weaker the coupling, the flatter and wider the probability distribution. The waiting time distribution also depends on the regional prevalence (Fig. 1b), which for measles ranged from 0.003 to 0.31% with a mean of 0.06% (median = 0.04%) before mass-vaccination; the

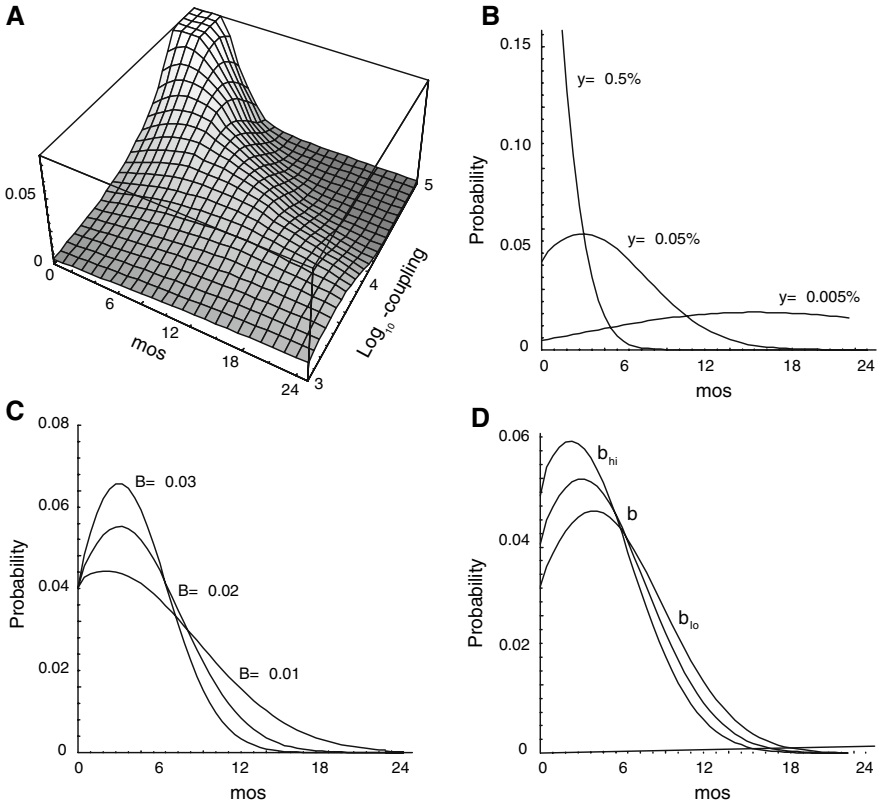

Fig. 1 The theoretical waiting times ('fade-out lengths') between outbreaks as predicted by Eq. 8. The waiting time distributions depends on (**a**) spatial coupling, (**b**) the regional prevalence of infection, (**c**) the annual *per capita* birth rate, and (**d**) the transmission rate

per capita birth rate (Fig. 1c) because this determines the rate of susceptible build-up; and the transmission rate (Fig. 1d): waiting times should be truncated during school terms, when transmission is enhanced, as compared to holidays when transmission is relatively low. Four important conclusions emerge from these theoretical explorations. First, while the details of demography (such as host birth rates) and transmission (such as term-time forcing) do affect the waiting time distributions, they should be much less important than the several orders-of-magnitude variation in regional prevalence. Second, any demographic and transmission variability may be swamped by variation in spatial coupling among the communities (Fig. 1a). This effect will be shown to be very important by the statistical estimates of coupling that we present in Sect. 5. Third, in contrast to simple time-invariant random processes, which give rise to exponential waiting-time distributions, fade-out distributions have their mode away from zero. The deficits at short waiting times result from initially low susceptible numbers because of depletion by previous epidemics: A new epidemic is only likely to take hold once susceptibles build up through subsequent births. Fourth—in summary—to predict fade-outs we need, at least, to consider (i) regional prevalence, (ii) spatial coupling, and (iii) the density of local susceptibles.

4 Empirical hazards

The probability calculations present clear hypotheses about how the hazard depends on local susceptible density, regional prevalence and, possibly, local community size if spatial coupling depends on size. In the case of our epidemic binomial variate, which flags whether or not a fade-out ends ('*success*') or continues ('*failure*') in any given time-step, we can use nonparametric logistic regressions to test for these hypothesized functional relationships. We used a nonparametric logistic regression (using a 2D-spline with 4 equivalent-degrees-of-freedom), a binomial error and a logit link (Hastie and Tibshirani 1990). To enhance power—particularly for large cities with scarce and rather brief fade-out periods—we grouped the data for the 20 communities closest to the target sizes of 2,000, 10,000, 50,000 and 200,000 inhabitants. In order to minimize the effect of underreporting, we discarded the initial two observations in each fade-out (Bartlett 1960; Grenfell and Bolker 1998) before calculating the empirical hazard functions. In this way, the singleton zero-incidence weeks that may represent underreporting during deep troughs rather than true fade-outs will not unduly bias the analysis. Figure 2 confirms how—for a given host community size—the hazard of sparking an epidemic is a function of the proportion of susceptibles and the regional infection level. The hazards further appear to asymptote for high susceptible and regional infective densities. Moreover, the asymptotic probability is an increasing

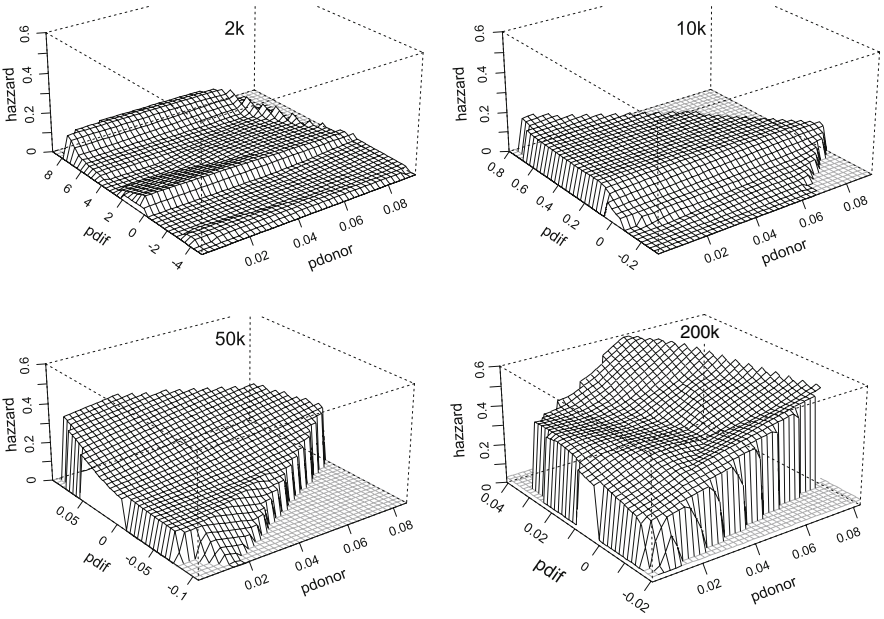

Fig. 2 The empirical hazard of ending a fade-out (and sparking of a new epidemic) as a function of proportion of local susceptibles and proportion of regional infecteds. The empirical hazards are split by local community size. The empirical hazard is estimated using a nonparametric logistic regression

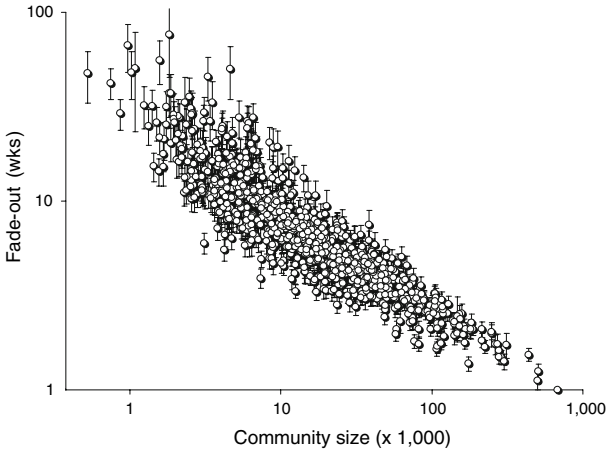

Fig. 3 The average fade-out length (±1 SD) during 1944–1965 for the 954 urban communities in England and Wales

function of local community size. This suggest that larger communities are, as may be expected, less isolated than smaller ones.

National notification was made mandatory by the UK Registrar General (OPCS) in 1940 in England and Wales (Fine and Clarkson 1982). With allowance for the under-reporting, the weekly data are complete for the 945 cities and towns in England and Wales (Grenfell and Bolker 1998). We focus on the data from 1944 (after the major perturbations of World War II) until mass-vaccination started in 1967. Figure 3 shows the average fade-out length as a function of community size. Two key points are apparent: (i) the average fade-out length follows a tight inverse relationship with community size; and (ii) the variance in the fade-out length (reflected in the error bars) are progressively wider in smaller communities, mirroring the widened theoretical waiting-time distributions as coupling decreases (Fig. 1).

As the theory predicts, the consequence of the greater isolation and slower susceptible replenishment of smaller communities is less frequent outbreaks and longer fade-outs. This, of course, was presciently recognized in Bartlett's sequence of seminal papers on the stochastic theory of measles epidemics (Bartlett 1956, 1957, 1960).

5 Estimating spatial coupling

Conditional on the data on susceptibles and the regional prevalence of infection, we can combine the theoretical hazard model (Sect. 3) with standard likelihood theory to estimate the spatial contact rate, c—a hitherto elusive parameter in epidemiology. The theoretical waiting time distribution may be seen as representing the expectation of a binomial process for which the log-likelihood of the fade-out data is given by:

$$\ell(c_j|I_{t-1,j}=0)=\sum_{I_{t-1,j}=0}\ln\left(\hbar_{t,j}^{z_{t,j}}(1-\hbar_{t,j})^{1-z_{t,j}}\right), \tag{9}$$

where $z_{t,j}$ is one if $I_{t,j} > 0$ and zero otherwise, and $\hbar_{t,j}$ is given by Eq. 7. The associated score function, $U = \partial\ell/\partial c$, and Fisher information, $i = -\partial^2\ell/\partial c^2$, are:

$$U(cj) = \sum_{I_{t-1,j}=0} \frac{x\,\overline{y}\,\left(S\,\beta + e^{c\,x\,\overline{y}}\,(z - S\,\beta + S\,z\,\beta)\right)}{\left(e^{c\,x\,\overline{y}} - 1\right)\,\left(e^{c\,x\,\overline{y}} + S\,\beta\right)}, \tag{10}$$

and

$$i(cj) = \sum_{I_{t-1,j}=0} \frac{e^{c\,x\,\overline{y}}\,x^2\,\overline{y}^2\,\left(2\,e^{c\,x\,\overline{y}}\,S\,\beta + S\,\beta\,(z + S\,z\,\beta - 1) + e^{2\,c\,x\,\overline{y}}\,(z - S\,\beta + S\,z\,\beta)\right)}{\left(e^{c\,x\,\overline{y}} - 1\right)^2\,\left(e^{c\,x\,\overline{y}} + S\,\beta\right)^2}, \tag{11}$$

respectively, where all symbols are as defined in Eq. 7. Note that subscripts are suppressed in Eqs. 10 and 11. We use Newton–Raphson to solve for $U(c) = 0$ and find the maximum likelihood estimate of c. Following elementary likelihood theory (McCullagh and Nelder 1989), we calculate its asymptotic standard error as $\mathrm{se}(\hat{c}_j) = i^{-1}(\hat{c}_j)$.

The estimates of spatial coupling reveal a tight relationship with community size (Fig. 4a; $\log(c) = 0.69 + 0.98\log(size)$, $p < 0.01$, $R^2_{adj} = 0.83$). Note that the confidence limits blow up for the largest communities, because these experience so few and short fade-outs that the statistical power becomes very low. The scaling of c is likely to be because of the many more susceptibles that can potentially get in contact with regional infecteds in large communities; On a per susceptible basis there appears to be no relationship between coupling and community size (Pearson correlation $= 0.04$, $p = 0.21$).

The residuals around the log-linear relation (Fig. 4b) reveals some geographically conspicuous features. The communities in Cornwall and southwestern Wales are consistently more isolated than expected from their population sizes alone. In contrast, the communities around London and in the industrial northwest are much less isolated than expected from their sizes. Interestingly, the latter two centra have previously been shown to be the foci from which waves of infection emanates (Grenfell et al. 2001). Hence, our statistical analysis should allow the construction of relative and absolute risk maps for disease spread.

6 Discussion

The spatial dimension is increasingly recognized as crucial to the dynamics and persistence of acutely infectious pathogens. This is because the epidemic outbreaks that result from rapid contagion are usually followed by deep troughs in prevalence during which extinction of the disease-causing agent is certain in all but the largest of host communities. Recently, significant insights into the dynamics of such pathogens have been garnered through application of the principles of metapopulation ecology, which explicitly considers how regional prevalence depends on rates of local extinction and reinvasion (Keeling et al. 2004). Childhood diseases, such as measles, represent the

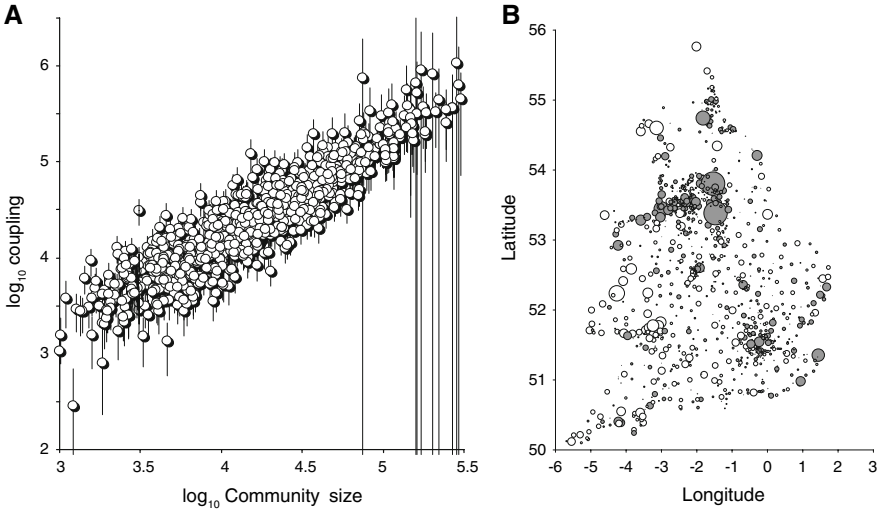

Fig. 4 (**a**) The estimated strength of spatial coupling (with 95% confidence intervals) for the 954 urban communities in England and Wales. (**b**) The residuals from the regression $\log(c) = 0.69 + 0.98\log(size)$ plotted at their geographic coordinates. Positive values are shaded with grey, negative values are open

archetype, here, because the complete protection awarded to recovered individuals leads to particularly deep troughs (Grenfell and Bjornstad 2005). In this paper we detail how stochastic process theory provides additional insights and allows for estimation of spatial epidemiological parameters.

The basic notions we present are not new; Almost 50 years ago, Bartlett (1956, 1957, 1960) identified the critical community size for measles persistence and proposed that the fade-outs represent realizations of epidemiological waiting time processes. Our refined insights results from our spatio-temporally exhaustive data set (Grenfell et al. 2001), the recent advances in susceptible reconstruction, and more detailed descriptions of the seasonality and scaling of transmission (Bjørnstad et al. 2002; Grenfell et al. 2002). In combination, the theory, data and statistics lay bare how—perhaps as may be expected—big host communities are more strongly coupled to the metapopulation at large. Beyond this, the communities around central conurbations appear to be of disproportionate importance in the spatial transmission. Not coincidentally, the most conspicuous areas of above-average coupling corresponds to the two previously identified regions from which waves of infection emanates (Grenfell et al. 2001). Together, the isolation of smaller communities and the deficit of susceptibles at the beginning of each fade-out explain the conspicuous deviation from exponential waiting times in the fade-out distributions, and the inverse (log-)relationship between average fade-out lengths and community size.

In this study, we have developed a theory of epidemic risk from the point of view of local recipient communities embedded in a regional metapopulation for which we assume we do not need to consider explicit spatial locations. Ultimately, we will want to explicitly infer the transportation network among all communities. An unconstrained network would require estimation of the strength of coupling for each of the

$p(p-1)/2$ pair-wise links between p local communities. This, of course, is not feasible for the 954 communities in England and Wales given that we cannot observe spatial transmission directly, but only its consequences when new outbreaks are sparked. Insights into the spatial network of spread can be garnered from detailed sociological (Eubank et al. 2004) and transportation data (Guimera and Amaral 2004). However, we believe that statistical fitting of simple models—here for the coupling between urban centers—may provide additional insights. For instance, gravity models from transportation theory (Erlander and Stewart 1990; Cliff et al. 1993; Xia et al. 2004) may provide a fruitful area for future research.

Acknowledgements This work was supported by grants from the Fogarty International Center of the NIH (ONB and BTG) and the Wellcome Trust (BTG).

References

Anderson RM, May RM (1991) Infectious diseases of humans: dynamics and control. Oxford University Press, Oxford

Bartlett MS (1956) Deterministic and stochastic models for recurrent epidemics. In: Neyman J (ed) Proceeding of the third Berkeley symposium on mathematical statistics and probability. University of California Press, Berkeley, pp 81–109

Bartlett MS (1957) Measles periodicity and community size. J R Stat Soc A 120:48–70

Bartlett MS (1960) The critical community size for measles in the U.S. J R Stat Soc A 123:37–44

Bjørnstad O, Finkenstädt B, Grenfell BT (2002) Endemic and epidemic dynamics of measles. I. Estimating transmission rates and their scaling using a time series SIR model. Ecol Monogr 72:185–202

Clark JS, Bjørnstad ON (2004) Population inference from messy data: errors, missing and hidden states, and lagged responses. Ecology 85:3140–3150

Cliff AD, Haggett P, Smallman-Raynor M (1993) Measles: an historical geography of a major human viral disease from global expansion to local retreat 1840–1990. Blackwell, Oxford

Erlander S, Stewart N (1990) The gravity model in transportation analysis – theory and extensions. Topics in Transportation. VSP, Utrecht

Eubank S, Guclu H, Kumar VSA, Marathe MV, Srinivasan A, Toroczkai Z, Wang N (2004) Modelling disease outbreaks in realistic urban social networks. Nature 429:180–184

Fine PEM, Clarkson JA (1982) Measles in England and Wales. I. An analysis of factors underlying seasonal patterns. Int J Epidemiol 11:5–15

Finkenstädt B, Grenfell B (2000) Time series modelling of childhood diseases: a dynamical systems approach. Appl Stat 49:187–205

Finkenstädt B, Bjørnstad ON, Grenfell BT (2002) A stochastic model for extinction and recurrence of epidemics: estimation and inference for measles outbreaks. Biostatistics 3:493–510

Glass K, Xia Y, Grenfell BT (2003) Interpreting time-series analyses for continuous-time biological models: measles as a case study. J Theor Biol 223:19–25

Grenfell B, Bjørnstad O (2005) Sexually transmitted diseases: epidemic cycling and immunity. Nature 433:366–367

Grenfell BT, Bolker BM (1998) Cities and villages: infection hierarchies in a measles metapopulation. Ecol Lett 1:63–70

Grenfell B, Harwood J (1997) (Meta)population dynamics of infectious diseases. Trends Ecol Evol 12:395–399

Grenfell BT, Bjørnstad ON, Kappey J (2001) Travelling waves and spatial hierarchies in measles epidemics. Nature 414:716–723

Grenfell BT, Bjørnstad ON, Finkenstädt B (2002) Endemic and epidemic dynamics of measles. II. Scaling noise, determinism and predictability with the time series SIR model. Ecol Monogr 72:185–202

Guimera R, Amaral LAN (2004) Modeling the world-wide airport network. Eur Phys J B 38:381–385

Hanski I, Gaggiotti O (eds) (2004) Ecology, genetics, and evolution of metapopulations. Elsevier, Amsterdam

Hastie TJ, Tibshirani RJ (1990) Generalized additive models. Chapman and Hall, London

Keeling MJ, Rohani P (2002) Estimating spatial coupling in epidemiological systems: a mechanistic approach. Ecol Lett 5:20–29

Keeling MJ, Bjørnstad ON, Grenfell BT (2004) Metapopulation dynamics of infectious diseases. In: Hanski I, Gaggiotti O (eds) Ecology, genetics, and evolution of metapopulations. Elsevier, Amsterdam, pp 415–445

Kendall DG (1949) Stochastic processes and population growth. J R Stat Soc B 11:230–264

Liu WM, Iwasa Y, Levin SA (1986) Influence of nonlinear incidence rates upon the behaviour of SIRs epidemiological models. J Math Biol 23:187–204

McCullagh P, Nelder JA (1989) Generalized linear models, vol 37 of Monographs on statistics and applied probability, 2nd edn. Chapman and Hall, London

Murray GD, Cliff AD (1975) A stochastic model for measles epidemics in a multi-region setting. Inst Br Geogr 2:158–174

Rand DA, Wilson HB (1991) Chaotic stochasticity: a ubiquitous source of unpredictability in epidemics. Proc R Soc Lond B 246:179–184

Rohani P, Keeling MJ, Grenfell BT (2002) The interplay between determinism and stochasticity in childhood diseases. Am Nat 159:469–481

Smith DL, Lucey B, Waller LA, Childs JE, Real LA (2002) Predicting the spatial dynamics of rabies epidemics on heterogeneous landscapes. Proc Natl Acad Sci USA 99:3668–3672

Xia Y, Bjørnstad ON, Grenfell BT (2004) Measles metapopulation dynamics: a gravity model for epidemiological coupling and dynamics. Am Nat 164:267–281

Author Biographies

Ottar N. Bjørnstad is a Professor in the Departments of Entomology and Biology, and Adjunct Faculty in Statistics, at the Pennsylvania State University. He holds an M.S. in Zoology and a PhD in Ecology from the University of Oslo. His primary research interests centers on dynamics and inference with respect to infectious diseases and other outbreaking pests.

Bryan T. Grenfell is a Professor in the Department of Biology at the Pennsylvania State University and a fellow of the Royal Society. He holds an M.S. in Biological Computation and a DPhil in Zoology from York University. Professor Grenfell is a population biologist, working at the interface between theoretical models and empirical data. He is particularly interested in understanding the spatio-temporal dynamics of infectious disease.